LBL-30273
UC-405

Lawrence Berkeley Laboratory
UNIVERSITY OF CALIFORNIA

EARTH SCIENCES DIVISION

Removal of Trichloroethylene Contamination from the Subsurface—A Comparative Evaluation of Different Remediation Strategies by Means of Numerical Simulation

A.E. Adenekan, K. Pruess, and R.W. Falta

December 1990

LOAN COPY
Circulates
for 4 weeks
Bldg. 50 Library.
LBL-30273
Copy 2

Prepared for the U.S. Department of Energy under Contract Number DE-AC03-76SF00098

DISCLAIMER

This document was prepared as an account of work sponsored by the United States Government. While this document is believed to contain correct information, neither the United States Government nor any agency thereof, nor the Regents of the University of California, nor any of their employees, makes any warranty, express or implied, or assumes any legal responsibility for the accuracy, completeness, or usefulness of any information, apparatus, product, or process disclosed, or represents that its use would not infringe privately owned rights. Reference herein to any specific commercial product, process, or service by its trade name, trademark, manufacturer, or otherwise, does not necessarily constitute or imply its endorsement, recommendation, or favoring by the United States Government or any agency thereof, or the Regents of the University of California. The views and opinions of authors expressed herein do not necessarily state or reflect those of the United States Government or any agency thereof or the Regents of the University of California.

LBL-30273

Removal of Trichloroethylene Contamination from the Subsurface— A Comparative Evaluation of Different Remediation Strategies by Means of Numerical Simulation

A. E. Adenekan, K. Pruess, and R. W. Falta

Earth Sciences Division
Lawrence Berkeley Laboratory
University of California
Berkeley, California 94720

December 1990

This work was supported by the U.S. Department of Energy under Contract No. DE-AC03-76SF00098.

Introduction

Volatile organic compounds such as petroleum hydrocarbons and halogenated hydrocarbon solvents are common contaminants of the subsurface environment. Although immiscible with water, many of these organics have large enough aqueous phase solubilities to significantly degrade the quality of groundwater with which they come in contact. In addition, many of these substances exhibit high vapor pressures, causing them to partition strongly into the gas phase in their surroundings. Because of these properties, a volatile organic compound (VOC), once introduced into the subsurface may be transported as a solute, a vapor, or as a constituent in a non-aqueous phase liquid (NAPL). This implies that at some sites, an adequate description of the migration of these contaminants in the subsurface would necessarily involve three phases—gas, aqueous and NAPL. For example, to design an effective aquifer remediation scheme for a site where NAPL is present, it would be wrong to focus solely on the aqueous phase while ignoring either the gas phase or the NAPL phase.

Equations governing multiphase fluid flow with interphase mass transfer in porous media have been presented in the literature, see for example Faust [1985], Abriola and Pinder [1985], Falta [1990]. Owing to the highly non-linear nature of these equations, they are not amenable to solution by analytical means. As a result, significant research effort has been directed toward the development of numerical simulators capable of solving the system of equations and modeling the behavior of NAPL contaminants in the subsurface under natural (ambient) conditions, as well as in response to various clean-up and treatment procedures.

The capabilities and limitations of several of the numerical simulators reported in the literature have been reviewed and summarized by Falta [1990]. The interested reader should consult that reference. In the present work, we use a simulator developed by Falta *et al.* [1990a], known as "STMVOC," which models true three-phase flow in which NAPL, gas and aqueous phases can move in response to pressure, capillary and gravitational forces. STMVOC is capable of

handling three-dimensional, three-phase fluid flow with strong heat transport and the associated phase change effects. Heat transport occurs due to conduction and multiphase advection, taking into account both latent and sensible heats of the phases. Three components are considered in the present formulation of STMVOC: air (which is actually a pseudo-component), water and a volatile organic compound. These three components can be present in the three phases, with the distribution of any one component among the phases being subject to the constraint of local thermodynamic equilibrium. Transport of the three mass components occurs by advection in all three phases and by multicomponent diffusion in the gas phase. Mechanisms of interphase mass transfer for the organic chemical include evaporation and condensation of the NAPL, dissolution of the NAPL into the aqueous phase, and equilibrium phase partitioning between the gas, water and solid phases. Interphase mass transfer of the water component includes evaporation and condensation and interphase mass transfer of the air component consists of equilibrium partitioning between the gas, NAPL and aqueous phases. Falta *et al.* [1990a] give a detailed description of the mathematical formulation of STMVOC. The simulator has been partly validated with several one- and two-dimensional laboratory experiments in which NAPL was displaced by injecting steam (Hunt *et al.*, 1988; Basel and Udell, 1989; Falta *et al.*, 1990a,b).

In the work reported here, we use the STMVOC simulator to evaluate the feasibility and effectiveness of various remedial strategies that one might consider when subsurface contamination due to a VOC spill occurs. This evaluation is carried out in the context of an idealized problem, with parameters chosen so as to make it generically relevant to the conditions at a real hazardous waste site—the Savannah River Site (SRS) in Aiken, South Carolina.

Below we discuss some of the important hydrologic features of the SRS site and those aspects of the site history that are known to us. This type of background information should make it easier to see the logic behind some of our choices of parameters for the idealized problem.

BACKGROUND

Recent hydrogeologic investigations at the Savannah River Site have shown that groundwater beneath the M-Area of the plant is contaminated with VOCs, primarily trichloroethylene (TCE) and tetrachloroethylene (PCE). Some reports (for example Kaback *et al.*, 1989) suggest that the contamination resulted from the leakage of waste solvents from a process sewer line into the subsurface.

Some remedial activities have taken place at the site. Between September 1985 and September 1986, groundwater was pumped at an average rate of about 10 million gallons per month from eleven recovery wells in the M-Area. The water was treated in an air stripper and then discharged to an NPDES permitted outfall located south of the site. Colven *et al.* [1987] estimated that more than 53,000 pounds of VOCs were removed from the groundwater during that period.

It is known that "residual concentrations of VOCs in the vadose zone provide a continuous source of contaminants to the groundwater" (Kaback *et al.*, 1989). Therefore, some effort is now being directed at exploring other remedial methods that address the vadose zone contamination. One remedial method being considered for use at the site is in-situ air stripping in the form of air injection below the water table and air extraction from the vadose zone. For this purpose, two horizontal wells were installed in the M-Area during September and October 1988. One well (AMH-2), located 25 m below the ground surface is above the water table. The other well (AMH-1) lies below the water table at a depth of about 55 m below the ground surface. Details of the construction and completion of these wells were presented by Kaback *et al.* [1989].

HYDROGEOLOGIC SETTING

According to the descriptions of Kaback *et al.* [1989] and Colven *et al.* [1987], unconsolidated sediments beneath the site consist of alternating sand, clayey sand and generally discontinuous clay layers. Locally, the uppermost five water-bearing units that have been delineated are of sands that are moderately sorted, ranging from fine- to coarse-grained and have been named

(starting from the top):

1) the Water Table unit;

2) the Upper Congaree unit;

3) the Lower Congaree unit;

4) the Ellenton Sand unit; and

5) the Black Creek unit.

The Black Creek unit is located approximately 100 m below the ground surface.

Groundwater conditions near the site reflect the fact that the SRS is located on a topographic high—the Aiken Plateau. Flow in the Water Table and Ellenton Sand units is primarily downward, while flow in the Congaree units is towards Upper Three Runs Creek, and flow in the Black Creek unit is towards the Savannah River (Haselow, *private communication*, 1991). The groundwater table is about 40 m below the ground surface. For purposes of numerical modeling, natural groundwater flows were neglected, and the model system was initialized as being in static gravity-capillary equilibrium (see below).

The data reported by Colven *et al.* [1987] on groundwater VOC concentrations below the water table showed local concentrations of TCE and PCE as high as 300 mg/l. TCE concentrations in the saturated zone near well AMH-1 are smaller, on the order of 1 mg/l (Haselow, *private communication*, 1991). The aqueous solubilities of TCE and PCE are about 1100 mg/l and 300 mg/l, respectively. Therefore, the reported PCE concentrations suggest the presence of PCE in the subsurface as a separate phase. The fact that the reported TCE concentrations are below the solubility limit does not necessarily imply the absence of a non-aqueous TCE phase. Because of formation heterogeneities, it is possible that the TCE distribution may be quite non-uniform. Furthermore, aqueous solubilities are normally discussed in the context of a pure solute. When dealing with a mixture of solutes (like a mixture of TCE and PCE), the equilibrium aqueous concentration of each solute will be lower than its solubility by a factor (less than 1) related to its mole fraction in the mixture.

Near the suspect sewer line, more than fifteen monitoring wells screened in the water table aquifer, covering an area of about 0.3 square miles had TCE and PCE concentrations in excess of 0.1 mg/l. A similar distribution of VOCs was reported for the Upper Congaree unit. Much lower concentrations were reported for the lower sand units. Colven *et al.* [1987] estimated that more than 95 percent (by mass) of the dissolved VOCs is within the Water Table and Upper Congaree units.

NUMERICAL MODEL

The work described in this report is based on a two-dimensional (2-D) vertical cross section model. The model has two horizontal layers with different hydraulic properties, based on those reported for the two upper sand layers at the SRS site. The bulk of the dissolved VOC at the SRS was found in the two upper sand layers, so that such a model will be relevant to the problem at that site. The upper and lower layers were assigned thicknesses of 45 m and 15 m, respectively.

Figure 1 shows the dimensions of the flow model, the two soil layers represented in the model and the finite difference grid. The position of the water table shown corresponds to the average water table depth recorded for the SRS site. The horizontal extent of the model was taken to be 475 m. We estimated that this distance should be sufficient for the effect of perturbations from remediation operations applied at one end to dissipate and therefore not affect conditions at the other end. The smallest grid blocks are 5 m by 5 m, while the largest are 5 m by 50 m. This gridding resulted in a total of 300 elements in the computational domain. A horizontal thickness of 1 m was specified, consistent with a 2-D model. To relate this 2-D model to the SRS site, we note that based on site plans made available to us, approximately 500 m of the suspect sewer line traverses the contaminated portion of the site. The plans and other data also indicate that the lengths of the horizontal portions of the lower well AMH-1 and upper well AMH-2 are about 100 m and 40 m, respectively, and that the alignment of the horizontal portion of each well closely follows that of the sewer line. The vertical section represented in our model can therefore be viewed as perpendicular to the alignment of the sewer line.

Model Parameters

The hydrologic properties of the model system are specified in Table 1. The basis for our choices of the most important parameter values is discussed below.

Permeability

The upper layer was assigned a permeability of 3.24×10^{-12} m^2 and a permeability of 1.58 $\times 10^{-11}$ m^2 was specified for the lower layer. These values correspond to those used in earlier flow models of the SRS site (Colven *et al.*, 1987). Each layer was taken to be isotropic with respect to permeability.

Porosity

A uniform porosity of 0.35 was specified for each of the two layers. This is based on estimates of Kaback *et al.* [1989] for soils found at the SRS site. They calculated total porosity from grain size analyses according to the method of Beard and Weyl [1973].

Capillary Pressure Function

For the simulations described below, we specified a 3-phase capillary pressure function based on the method proposed by Parker *et al.* [1987]. In that formulation, the NAPL-water capillary pressure P_{cnw} is assumed to be a function only of water saturation S_w, while the gas-NAPL capillary pressure P_{cng} is assumed to be a function only of gas saturation S_g. Closed-form equations were given for these two capillary functions:

$$P_{cnw} = \frac{\rho_w g}{\alpha_{nw}} \left[\left[\frac{S_w - S_m}{1 - S_m} \right]^{-1/m} - 1 \right]^{1/n} \tag{1}$$

$$P_{cgn} = \frac{\rho_w g}{\alpha_{gn}} \left[\left[\frac{S_w + S_n - S_m}{1 - S_m} \right]^{-1/m} - 1 \right]^{1/n} \tag{2}$$

where $m = 1 - 1/n$ and n, α_{nw}, α_{gn}, and S_m are empirically determined constants. The values of constants α_{nw}, n, and S_m used in these equations were those reported by Parker *et al.* [1987] which were based on measurements made in a sandy porous medium (see Table 1). No reliable

data on α_{gn} were found in the literature. We performed a series of test runs in which we studied the sensitivity of the model results to the value of α_{gn}. If α_{gn} was chosen such that P_{cgn} took on non-zero values of magnitude similar to P_{cnw}, the NAPL injected at the ground surface moved both downward and laterally outward at about the same rate. This is believed not to be a physically realistic behavior except in a layered medium in which vertical permeability is substantially lower than horizontal permeability. Accordingly, we set $P_{cgn} = 0$ in the present study.

With P_{cnw} and P_{cgn} determined from the equations above, the gas-water capillary pressure P_{cgw} is calculated from

$$P_{cgw} = P_{cgn} + P_{cnw} \tag{3}$$

Relative Permeability Functions

The three-phase relative permeabilities for the gas and water phases were calculated based on the widely accepted premise that the gas phase relative permeability depends only on the gas phase saturation, and that the water phase relative permeability depends only on the water phase saturation. This corresponds to water being the wetting phase, gas the non-wetting phase and the NAPL having intermediate wettability. Water phase and gas phase relative permeabilities in a three-phase system (k_{rw} and k_{rg}) are therefore calculated the same way as in two-phase flow. Two-phase experimental data have been successfully fitted with functions of the form

$$k_{rw} = \left[\frac{S_w - S_{wr}}{1 - S_{wr}} \right]^n \tag{4}$$

$$k_{rg} = \left[\frac{S_g - S_{gr}}{1 - S_{gr}} \right]^m \tag{5}$$

where S_{gr} and S_{wr} are the irreducible saturation of gas and water, respectively and n and m have values between 2 and 4. The simulations described below were based on $S_{gr} = 0.01$, $S_{wr} = 0.10$ and $n = m = 3.0$

The first method of Stone [Stone, 1970] was used to calculate the NAPL relative permeability. In this method, the NAPL relative permeability, k_{rn}, is considered to be a function of both the

water and gas saturations, and is calculated from the two two-phase relative permeability functions in a NAPL/water and a gas/NAPL system. With the modification by Aziz and Settari [1979], Stone's first method is written as

$$k_{rn} = k_{rncw} S_n^* \beta_w \beta_g \tag{6}$$

where

$$\beta_w = \frac{k_{rnw}(S_w)}{k_{rncw}(1 - S_w^*)} \tag{7}$$

and

$$\beta_g = \frac{k_{rng}(S_g)}{k_{rncw}(1 - S_g^*)} \tag{8}$$

k_{rnw} in (7) is the NAPL relative permeability function in a two-phase NAPL/water system. In (6), (7) and (8), k_{rncw} is the NAPL relative permeability in the presence of irreducible water (no gas phase in the system). The two-phase gas-NAPL relative permeability k_{rng} required by (8) is assumed to have been measured in the presence of this irreducible water. With this assumption and through the use of k_{rncw}, the three-phase NAPL relative permeability will reduce to the appropriate two-phase relationship if two-phase conditions are present. The reduced phase saturations needed in (6), (7) and (8) are

$$S_n^* = \frac{S_n - S_{nr}}{1 - S_{wr} - S_{nr}} \tag{9}$$

$$S_w^* = \frac{S_w - S_{wr}}{1 - S_{wr} - S_{nr}} \tag{10}$$

and

$$S_g^* = \frac{S_g}{1 - S_{wr} - S_{nr}} \tag{11}$$

where S_{nr} is the irreducible NAPL saturation, and S_{wr} is the irreducible water saturation. In this study, S_{nr} and S_{wr} were taken to be 0.05 and 0.10 respectively. The tortuosity factor for gas phase diffusion was taken as $\tau = \phi^{1/3} S_g^{7/3}$.

Fluid Properties

The simulations reported here are based on the assumption that TCE is the only component of the contaminant. Thermophysical properties of TCE such as viscosity, density, enthalpy, etc. vary with temperature and pressure and are calculated in STMVOC using the corresponding-states method. Thermophysical properties of the gas and aqueous phases generally depend on temperature, pressure and composition and are calculated internally by STMVOC. The various constants used to calculate properties of TCE are listed in Table 2.

Numerical Simulations

In this section, we present a description and discussion of the results of the different simulations that were performed in this study (see Table 3). The first three simulations described below were performed in order to prepare a set of initial conditions for the latter three simulations which represent different remediation alternatives.

Simulation No. 1: Gravity-capillary Equilibrium

This simulation was performed to develop initial conditions for a subsequent simulation. For this simulation, there is no TCE present in the system. A schematic of the vertical cross section modeled is shown in Figure 1. In order to achieve the desired gravity-capillary equilibrium, the system was initialized in two-phase conditions, with boundary conditions of atmospheric pressure (taken as 101 kPa) and a temperature of 20°C at the top (along A-B in Figure 1), a hydrostatic pressure corresponding to the desired elevation of the water table at the bottom (along D-C) and no-flow conditions at the lateral boundaries (A-D and B-C). The simulation was run until the system reached steady state, which corresponds to hydraulic and thermal equilibrium. In the subsequent simulations, these equilibrium initial conditions were maintained as boundary conditions at the right boundary (Figure 1).

Simulation No. 2: TCE Injection

In this simulation, liquid TCE was injected into the top left corner element at a rate of 1.173

$\times 10^{-4}$ kg/s. This is equivalent to the release of a standard barrel of TCE per month per lineal meter. This injection phase lasts for a period of 10 years, with a total release of 36,991 kg.

No-flux conditions were specified at the left and lower boundaries. At the right boundary, pressure and temperature were held constant at the values that resulted from the gravity equilibrium simulation. Atmospheric pressure and a temperature of 20°C were imposed at the upper boundary. These boundary conditions are shown in Figure 1. Unless otherwise stated, these are the same boundary conditions specified for all the other simulations described below. The result of the gravity equilibrium simulation was specified as the initial condition for this simulation.

In the unsaturated zone, liquid TCE travels vertically downwards under the force of gravity. Because of the assumption that $P_{cgn} = 0$ and because the water in this zone is essentially at a uniform saturation (the residual saturation), capillary forces present very little resistance to this downward motion of TCE. Below the water table, gravity is still the dominant force that controls the movement of the TCE, which at ambient conditions has a density of $\rho_{TCE} = 1462\ kg/m^3$ as compared to $\rho_{H_2O} = 998.1\ kg/m^3$. However, capillary forces are more important than they were in the unsaturated zone. The capillary pressure between the aqueous and TCE phases acts to oppose gravity, contributing to making the downward movement of the TCE somewhat slower than it was in the unsaturated zone. For example, simulation results show that for a given distance, the TCE travel time below the water table is about 15 percent longer than in the unsaturated zone. This is in spite of the higher permeability material below the water table.

When an impermeable layer is encountered (the lower boundary of the model in this case), the TCE begins to spread laterally. This movement is due to a lateral pressure gradient in the TCE. Because $\rho_{TCE} > \rho_{H_2O}$, on any given horizontal plane, the pressure will be greatest directly beneath the injection area as long as TCE saturation is above residual in some region directly above that plane. This lateral movement is however slower than the vertical movement of TCE either above or below the water table. At the end of the 10 years of injection simulated here, a separate TCE phase had spread along the impermeable bottom of the model over a lateral distance of about 45 m from the source (see Figure 2). The TCE inventory in our model may be

considerably larger than what is found near the horizontal wells at the Savannah River Site (Haselow, *private communication*, 1991).

Volatilization and subsequent migration in the gas phase are important when dealing with the transport of VOCs in the vadose zone. This simulation showed that, in addition to molecular diffusion, density-driven advection is also important in the gas phase transport of TCE. Falta *et al.* [1989] had demonstrated this effect for VOCs with vapor densities greater than that of air. Figure 3(a) shows the time evolution of the TCE concentration in the gas phase; the concentration contour with $C_g^{TCE} = 0.1$ kg/m^3 corresponds roughly to 80,000 ppm TCE by weight. Similar information is presented on Figure 3(b) for $C_g^{TCE} = 5.0 \times 10^{-5}$ kg/m^3 (approximately 40 ppm by weight). Over the 10-year injection period, the 0.1 kg/m^3 contour shifts laterally by about 80 m. Henry's Law dictates that groundwater in that vicinity would have a TCE concentration of 0.25 kg/m^3 (250 ppm), assuming thermodynamic equilibrium between the phases. In light of this, it is not difficult to see the threat which vadose zone contamination poses to groundwater far away from a NAPL spill even when the amount of spillage is such that the NAPL does not reach the water table.

Simulation No. 3: No Active Remediation for 25 Years after TCE Release had Stopped

Using the results obtained at the end of the 10-year injection phase as the initial condition, we simulated the system response over a 25-year period during which no active remedial action is taken. While we do not know the complete history of the SRS site, there are indications that most of the VOC release appears to have taken place more than 15 years ago (Haselow, *private communication*, 1991). This simulation was an attempt to represent the changes in contaminant distribution that occur during such a period of inactivity.

During this simulation period, the TCE continued its lateral movement above the lower boundary of the system, the NAPL advancing by another 42 m to about 87 m from the left boundary (see Figure 2). This represents a rate of movement that is slower than that estimated for the previous 10-year period. Unlike the previous 10-year period during which some lateral move-

ment of TCE occurred between grid-blocks that were not directly above the model's lower boundary, all the lateral movement in this "no-action" simulation occurred between grid blocks that lie directly above the impermeable lower boundary. Both of these effects are due to the fact that once the injection is stopped, the driving force for TCE movement is significantly reduced.

As shown in Figures 3(a) and 3(b), for a given concentration C_g^{TCE} of TCE in the gas phase, the speed of lateral displacement of the contour of that concentration decreases with distance from the source area. Although this behavior is typical of diffusion processes, it is more pronounced here for the following reason. One of the conditions imposed at the upper boundary of the model is that $C_g^{TCE} = 0$. Therefore in the region close to the source, there is a large upward concentration gradient which causes an upward diffusive flux, thus reducing the lateral migration of the "front."

The results also show that volatilization and the accompanying molecular diffusion alone are not enough to remove a NAPL from the soil even when such processes take place over a long period of time. This conclusion is supported by observations at the Savannah River Site (Haselow, *private communication,* 1991). Over the 25-year period simulated here, separate-phase TCE had been removed only from the uppermost of the grid blocks which had TCE initially, and this is because that uppermost grid block is directly connected to a boundary grid block in which $C_g^{TCE} = 0$.

Overall, of the 36,646 kg of TCE in place at the end of the 10-year injection period, only 1,049 kg (representing 2.8 percent) was removed due to volatilization and diffusion out of the surface during this 25 year "no-action" period.

Simulations representing remediation alternatives

Three remedial schemes were considered in the present study: vadose zone gas extraction, groundwater extraction, and combined air injection into the saturated zone and vadose zone gas extraction.

In each case, conditions at the end of the 25-year "no-action" period (35 years after the

start of TCE injection) were taken as initial conditions and each remediation simulation was carried out for a 5-year period. Note that these conditions are probably not representative of those encountered at the SRS site.

Simulation No. 4: Vadose zone gas extraction

In this simulation, gas was extracted from the vadose zone at the location of the upper horizontal well shown in Figure 1. This location corresponds to that of one of the two existing horizontal wells on the SRS site (AMH-2). Gas extraction from the corresponding grid block was based on a deliverability model which requires specification of a wellbore pressure, P_{wb} and a productivity index, PI. The simulator then calculates the mass rate of gas extraction, q_g from

$$q_g = \frac{k_{rg}}{\mu_g} \rho_g \cdot PI \cdot \left[P_g - P_{wb} \right] \tag{12}$$

where P_g, k_{rg}, μ_g and ρ_g are, respectively, the pressure, relative permeability, viscosity and density of the gas phase in the corresponding grid block. Note that for a well grid block that contains more than one phase at above residual saturation, an equation like (12) applies for the production rate of each phase. The productivity index (PI) is widely used in oil and geothermal reservoir modeling [Coats, 1977]. It is a function of medium permeability, size of the well grid block, and the skin factor and is calculated from

$$PI = \frac{2\pi k \Delta z}{\ln \frac{r_e}{r_w} + s - 1/2} \tag{13}$$

where $r_e = (\Delta x \Delta y / \pi)^{1/2}$ is an effective equivalent radius of the grid block containing the well, r_w is the well radius, Δx and Δy are the dimensions of the grid block normal to the axis of the well, Δz is the dimension of the grid block parallel to the well axis, k is the permeability and s is the skin factor. With $\Delta x = \Delta y = 5.0\,\mathrm{m}$, $\Delta z = 1.0\,\mathrm{m}$, $k = 3.24 \times 10^{-12}\,\mathrm{m}^2$ (corresponding to the permeability of the upper layer), $r_w = 3''$ and $s = 0$. PI was estimated (for half a well due to symmetry) to be $6.5 \times 10^{-12}\,\mathrm{m}^3$. In this simulation, P_{wb} was specified as 2/3 atm (67333.3 Pa). This, as well as the other assumed parameter values listed above resulted in a quasi-steady gas

extraction rate of about 0.004 kg/s per lineal meter of the well.

The simulation showed that all the separate-phase TCE in the vadose zone was volatilized in about 75 days. After the TCE had been volatilized, gas phase concentrations continued to decrease throughout the vadose zone, but the rate of decrease varied from one location to another. Figure 4 shows the locations of the $C_g^{TCE} = 1 \times 10^{-2}\ \mathrm{kg/m^3}$ contour at various times since the beginning of vadose zone gas extraction. C_g^{TCE} decreases quite rapidly in those parts of the system that are within the zone of influence of the extraction well (that is, those areas where the pressure is lowered due to the extraction well). This is due to the fact that advection is the dominant transport mechanism in such areas. This is not the case for those areas that are outside the zone of influence of the well. The rate of decrease of C_g^{TCE} in these areas is smaller. This is because the magnitude of advection is small and TCE leaves these areas mainly by diffusion. This diffusion is however augmented by the presence of the well since a higher concentration gradient in the direction of the well is maintained. This point is illustrated in Figure 4. The area enclosed by the $C_g^{TCE} = 1 \times 10^{-2}\ \mathrm{kg/m^3}$ contour decreases very rapidly for about 150 days following the start of gas extraction. This is because most of that area lies within the zone of influence of the well. At later times, the position of the contour changes more slowly because it moves beyond the zone that is strongly influenced by the well. The foregoing observation is not a limitation of this remediation method. It only highlights the fact that at a given site, more than one vadose zone gas extraction well may be required and that appropriate locations for the wells need to be determined.

On the other hand, the results show that this remedial scheme has almost no impact on the saturated zone. At the end of the 5-year gas extraction period, the distribution of the TCE below the water table remained essentially the same as it was at the beginning. Considering that TCE below the water table (both as NAPL and dissolved in the aqueous phase) represents about 88 percent of the total initial inventory of TCE, it is not difficult to see that vadose zone gas extraction is inadequate in this kind of situation. Curve A in Figure 5 is a plot of the cumulative mass of TCE removed from the system versus time. The rate of removal is very high initially and then

drops off to small values after all the separate-phase TCE in the vadose zone is volatilized.

Simulation No. 5: Groundwater Extraction

This is a simulation in which groundwater is extracted from the lower left corner of the mesh shown in Figure 1. The rate of extraction was based roughly on our knowledge of the pumpage that the aquifer underlying the SRS site was able to support during the "pump and treat" remediation period between September 1985 and September 1986. One set of three recovery wells each of which delivered 1 million gallons per month during that period are within 100 m of one another. If we assume that the horizontal well in the present simulation is 100 m long, extracting groundwater from this well at the same rate as those three recovery wells combined implies an extraction rate of 3.79 m^3/day per lineal meter of horizontal well. Because our model is symmetrical with respect to the left boundary, only half of this extraction rate, or 1.895 m^3/day per lineal meter, was used in this simulation. This extraction rate resulted in a drawdown of approximately 5 m at the well location at the end of 5 years.

Approximately 40 percent of the total TCE (i.e. both in the aqueous phase and as a separate phase) initially present below the water table was removed over the 5-year simulation period. The rate of removal varies with time as shown by curve B in Figure 5. That rate decreases with time, but not as rapidly as in the case of vadose zone gas extraction. Here, TCE removal rate continues to be appreciable at the end of 5 years.

Flow conditions in the system were such that TCE was removed both as a separate phase and in the dissolved form. However, the relative importance of these two forms of TCE removal varied with time and can be quantified in terms of a fractional flow defined as

$$f_{TCE} = \frac{volume\ flow\ rate\ of\ separate\text{-}phase\ TCE}{total\ volume\ flow\ rate\ of\ liquid}$$

The fractional flow is related to the relative magnitudes of pressure forces, capillary forces and dissolution rate. The magnitude of each of these varies with with distance from the well, and with time since extraction began. At any location below the water table, TCE saturation

decreases with time, so that NAPL relative permeability and f_{TCE} both decline. For this simulation, the fractional flow was about 0.02 at the beginning, 0.005 after 9 months and 0.001 at the end of the 5-year period. Based on an aqueous phase solubility of approximately 1,100 ppm, a fractional flow of 0.001 represents a condition in which the mass rate of removal of TCE in the dissolved form is approximately equal to the mass rate of removal as a separate phase. A value of $f_{TCE} << 0.001$ indicates that most of the TCE being removed from the system is in the dissolved form. If this simulation were continued, the fractional flow would continue to decrease until it became zero. This is the point at which TCE saturation is at, or below the residual saturation and thereafter TCE can only be removed from the system by dissolution in the aqueous phase. The steeper slope in the early part of curve B (Figure 5) results from the fact that TCE is being removed both as a separate phase and as a dissolved constituent in the aqueous phase. The slope decreases with time as the contribution of the separate-phase TCE decreases. Dissolved TCE is the main contributor in the latter part of the curve. Figure 6 shows the saturations of TCE at two different locations. At the location farther away from the well, the saturation decreased at an approximately uniform rate. This is because TCE was removed from that location primarily by dissolution—the initial saturation was not high enough for advection of the separate phase to be significant even at early times. At the other location (closer to the well), saturation decreased at a faster rate initially until advection of the separate phase became insignificant. The rate of decrease then approached that attributable to dissolution. These results show that extraction from below the water table is more efficient when the NAPL saturation is above residual. It should be noted that many hazardous organic chemicals are much less water-soluble than TCE, making removal in dissolved form a very slow process.

Conditions in the vadose zone were unaffected by this remediation scheme. Since TCE saturation in the vadose zone was initially less than residual, it could not be advected due to the gradient imposed by the extraction well. TCE concentrations in the gas phase remained high because separate-phase TCE was still present, and the gas phase pressure distribution in the vadose zone was hardly affected by the extraction well below the water table.

Simulation No. 6: Combined Air Injection and Gas Extraction

This represents a remediation scheme in which air is injected into the aquifer below the water table and simultaneously, gas is extracted from the vadose zone. The same well deliverability conditions as described under Simulation No. 4 were specified for the vadose zone extraction well. The mass rate of air injection into the saturated zone was made equal to the vadose zone mass extraction rate. The injected air was assigned thermodynamic properties that correspond to a temperature of 25°C and a pressure approximately equal to the quasi-steady pressure in the injection grid block. This pressure was determined in test runs to be about 4 bars. If one starts with air of say, 60 percent relative humidity at atmospheric pressure and 25°C and isothermally compresses it to 4 bars, the air will become vapor saturated (with some condensation occurring during this process). Based on this argument, the injected air was assigned a water vapor mass fraction corresponding to 100 percent relative humidity.

Results of this simulation show that its effectiveness in the vadose zone is similar to the case where there was only a vadose zone extraction well. The separate-phase TCE in the vadose zone was completely volatilized in about 60 days. Below the water table, it also took about 60 days to completely remove TCE from the injection grid block and neighboring grid blocks that were either directly above, or displaced horizontally but at a higher elevation than the injection well. TCE removal from adjacent grid blocks that were on the same horizontal plane as the injection well proceeded at a much slower rate. This result is shown in Figure 7. This difference is due to the geometry of the flow field induced by this arrangement. Because of buoyancy force on the injected gas, and the upward pressure gradient due to the relative positions of the injection and extraction wells, the hydraulic gradient is maximum in the vertical direction and the maximum gas phase flux is in this direction. Since the primary mechanism of TCE removal is volatilization by the flowing gas, the removal is quicker in those areas through which the flux of the gas phase is highest. The overall rate of TCE removal from the system is shown by curve C in Figure 5.

The flow field that results from the air injection was found to have an unfavourable effect

on the movement of the NAPL below the water table. The simulation shows that TCE was being advected laterally away from the injection well. This is due to pressure build-up at the well which causes a horizontal gradient in the direction away from the well. This pressure gradient is responsible for the slight increase in saturation at the farthest location shown in Figure 7. Over the 5-year simulation period, the horizontal extent of the NAPL had increased from 90 m to 100 m. Therefore, with regard to the saturated zone, this process is only effective in the immediate vicinity (on the order of 5 m) of the air injection well.

It should be pointed out that injection of gas below the water table gives rise to a gravitationally unstable displacement process. The injected gas would be expected to "finger" through limited regions from which it displaces the water. This fingering would diminish the contact between the NAPL/water and the gas, further reducing the rate of contaminant removal by volatilization. The spatial resolution of our grid is insufficient to resolve fingers, so that our simulation will overestimate TCE removal by volatilization beneath the water table.

Summary

Table 4 provides data that summarize the overall effectiveness of each remedial scheme described above. It is clear that neither vadose zone gas extraction nor groundwater extraction is adequate for the problem at hand. Each of these techniques focuses on either the saturated zone or the vadose zone, neglecting the other. It may appear that the natural thing to do is to combine these two techniques since they are complementary. However groundwater extraction is not very efficient when NAPL saturation is below residual, making it necessary for the operation to go on for up to twenty years or more at some sites. Also the cost of treating the large quantity of water extracted is prohibitive. For NAPLs having a very low solubility, groundwater extraction would not be an efficient means of removing low NAPL saturations [Hunt *et al.*, 1988a].

While gas extraction with air injection below the water table attempts to deal with both zones, it appears that its effectiveness in the saturated zone is quite limited. Some investigation regarding the stability of such a process is also necessary before it can be regarded as a viable alternative. A combination of groundwater extraction with air injection and gas extraction may

yield improved TCE removal.

A feature that makes air injection below the water table attractive is that TCE is removed from the saturated zone by volatilization, which is not limited by the residual saturation. The implication is that complete removal of TCE can potentially be achieved if enough contact or surface area is provided between the injected gas phase and the NAPL. An alternative method that shares this feature is steam flooding—both above and below the water table. Steam injection would cause VOCs present in the aquifer to volatilize and migrate in the gas phase under pressure gradients set up by injection and extraction wells. Some of the VOC may condense ahead of the steam front, forming a NAPL bank where the saturation and therefore the relative permeability may be high enough for NAPL to flow under the imposed pressure gradients. Steam flooding as a means of aquifer remediation appears promising and is presently under study with the STMVOC simulator.

Acknowledgement

The authors are indebted to Dr. John Haselow of Westinghouse Savannah River Company for his critical review of the manuscript and the suggestion of improvements. This work was supported by the U.S. Department of Energy under Contract No. DE-AC03-76SF00098.

References

Abriola, L. M. and G. F. Pinder, A multiphase approach to modeling of porous media contamination by organic compounds 1. Equation development, *Water Resources Research, 21*, (1), 11–18, 1985.

Aziz, K. and A. Settari, *Petroleum Reservoir Simulation*, Applied Science Publishers, London, 1979.

Basel, M. D. and K. S. Udell, Two dimensional study of steam injection into porous media, Multiphase Transport in Porous Media, ASME HTD vol. 127, 39–46, 1989.

Beard, D. S. and P. K. Weyl, Influence of texture on porosity and permeability of unconsolidated sand, *Am. Assoc. of Petrol. Geol. Bull., 57*, 349–369, 1973.

Coats, K. H., Geothermal reservoir modeling, Paper SPE 6892 presented at the 52nd Annual Fall Technical Conference and Exhibition of the SPE, Denver, CO, October, 1977.

Colven, W. P., L. F. Boone, J. G. Horvath and R. Lorenz, Effectiveness of the M–Area groundwater remedial action program, September 1985–September 1986. Report from E. I. Du Pont de Nemours and Company to the U. S. Department of Energy, February 1987.

Falta, R. W., Multiphase Transport of Organic Chemical Contaminants in the Subsurface, Ph.D. thesis, University of California, Berkeley, CA, 1990.

Falta, R. W., I. Javandel, K. Pruess and P. A. Witherspoon, Density-driven flow of gas in the unsaturated zone due to the evaporation of volatile organic compounds, *Water Resources Research, 25*, (10), 2159–2169, 1989.

Falta, R. W., K. Pruess, I. Javandel and P. A. Witherspoon, Numerical modeling of steam injection for the removal of nonaqueous phase liquids from the subsurface, 1. Numerical formulation, Lawrence Berkeley Laboratory Report LBL-29615, submitted to *Water Resources Research*, 1990(a).

Falta, R. W., K. Pruess, I. Javandel and P. A. Witherspoon, Numerical modeling of steam injection for the removal of nonaqueous phase liquids from the subsurface, 2. Code validation and application, Lawrence Berkeley Laboratory Report LBL-29616, submitted to *Water Resources Research*, 1990(b).

Faust, C. R., Transport of immiscible fluids within and below the unsaturated zone: A numerical model, *Water Resources Research, 21*, (4), 587–596, 1985.

Hunt, J. R., N. Sitar and K. S. Udell, Nonaqueous phase liquid transport and cleanup 1. Analysis of mechanisms, *Water Resources Research, 24*, (8), 1247–1258, 1988a.

Hunt, J. R., N. Sitar and K. S. Udell, Nonaqueous phase liquid transport and cleanup 2. Experimental studies, *Water Resources Research, 24*, (8), 1259–1269, 1988b.

Kaback, D. S., B. B. Looney, J. C. Corey and L. M. Wright, Well completion report on installation of horizontal wells for in-situ remediation tests, Report from Westinghouse Savannah River Company to the U. S. Department of Energy, August 1989.

Parker, J. C., R. J. Lenhard and T. Kuppusamy, A parametric model for constitutive properties governing multiphase flow in porous media, *Water Resources Research, 23*, (4), 618–624, 1987.

Stone, H. L., Probability model for estimating three-phase relative permeability, *Journal of Petroleum Technology, 22*, (1), 214–218, 1970.

Table 1. Formation parameters.

Parameter	Value
Permeability	
Upper layer	$k_1 = 2.24 \times 10^{-12}\ m^2$
Lower layer	$k_2 = 1.58 \times 10^{-11}\ m^2$
Total porosity	$\phi = 0.35$
Soil grain specific heat capacity	$C_R = 1000$ kJ/kg-°C
Soil thermal conductivity (dry)	$\lambda_D = 2.85$ W/m-°C
Soil thermal conductivity (wet)	$\lambda_W = 3.10$ W/m-°C
Soil grain density	$\rho_R = 2650\ kg/m^3$
Capillary pressure data (Equations 1 and 2)	
$S_m = 0.0$	
$n = 1.84$	
$\alpha_{nw} = 5.24\ m^{-1}$	
$m = 1 - 1/n$	
$g = 9.81\ m/s^2$	
$P_{cgn} = 0$	
Relative permeability data (Equations 4, 5 and 9)	
$S_{wr} = 0.10$	
$n = 3$	
$S_{gr} = 0.01$	
$m = 3$	
$S_{nr} = 0.05$	

Table 2. Constants for calculating thermophysical properties of TCE.

Constant	Value
Molecular weight	M_{wt} = 131.4 g/mole
Critical temperature	T_{crit} = 572.0 K
Critical pressure	P_{crit} = 50.5 bar
Critical compressibility	Z_{crit} = 0.265
Critical volume	V_{crit} = 256.0 cm^3/mole
Normal boiling point	T_b = 87.3°C (360.4 K)
Pitzer's acentric factor	ω = 0.213
Dipole moment	η_d = 0.9 debyes
Aqueous solubility	$\bar{c}_w^c$ = 1,100 mg/l
Reference liquid density*	ρ_{nR} = 1462.0 kg/m^3
Reference liquid viscosity*	μ_{nR} = 0.59 cP

* at T_R = 293 K, P_R = 1 bar

Table 3. Summary of simulation studies.

Site Condition	Simulation	Process	Duration
natural state	1	gravity equilibration	∞ (steady state)
contamination	2	TCE spill and infiltration	10 years
	3	no action (ambient diffusion and advection)	25 years
remediation	4	vadose zone gas extraction	5 years
	5	groundwater extraction	5 years
	6	vadose zone gas extraction with air injection beneath water table	5 years

Table 4. Effectiveness of remediation schemes.

Simulation* Process	#2 spill and infiltration	#3 no action	#4 gas extraction	#5 groundwater extraction	#6 gas extraction w/ air injection
TCE vapor (kg)	178.9	216.8	6.1	211.7	7.9
Dissolved TCE (kg)	213.5	299.8	259.7	272.6	221.0
Liquid TCE (kg)	36,254	35,080	31,019	21,151	25,315
Total TCE (kg)	36,646	35,597	31,285	21,635	25,544

*see Table 3

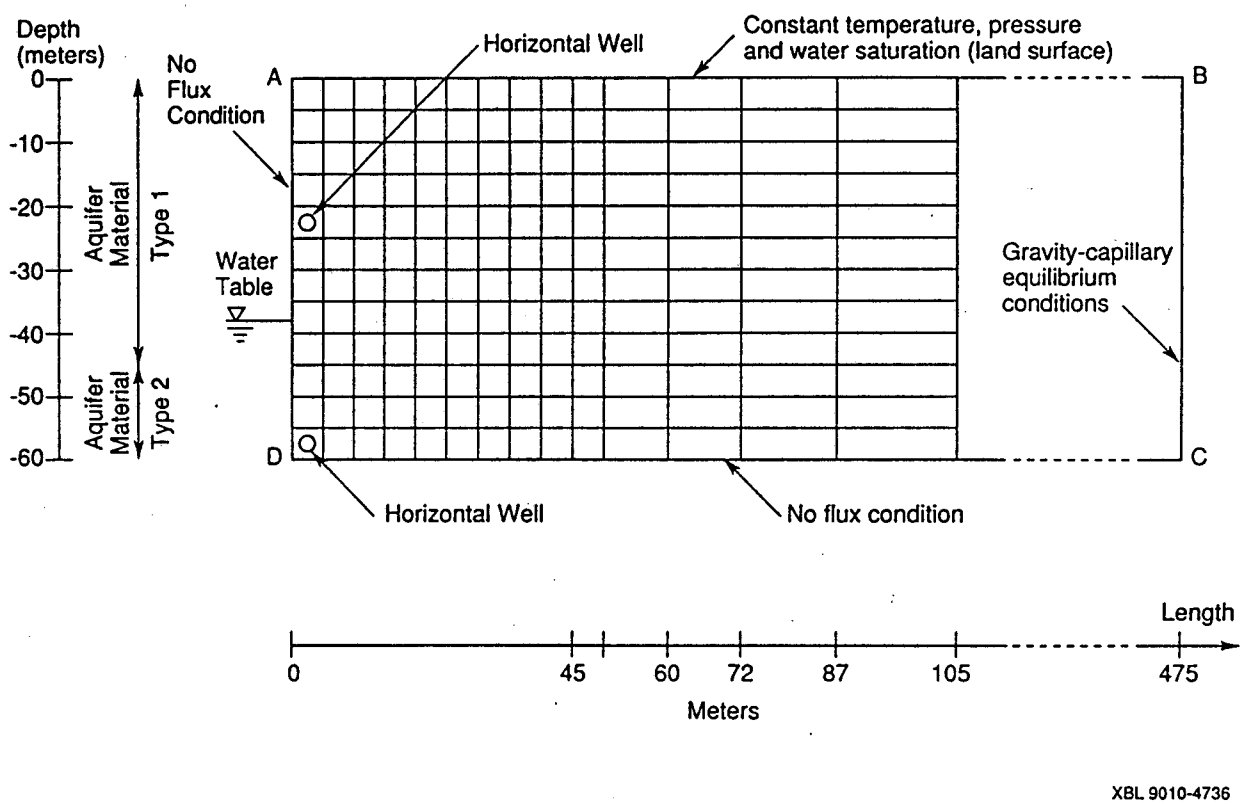

Figure 1. Schematic of the vertical cross section modeled in the simulations. Gridding and locations of horizontal treatment wells are shown. Boundary conditions are as applied for the simulation of contamination and remediation processes (simulations 2 through 6, Table 3).

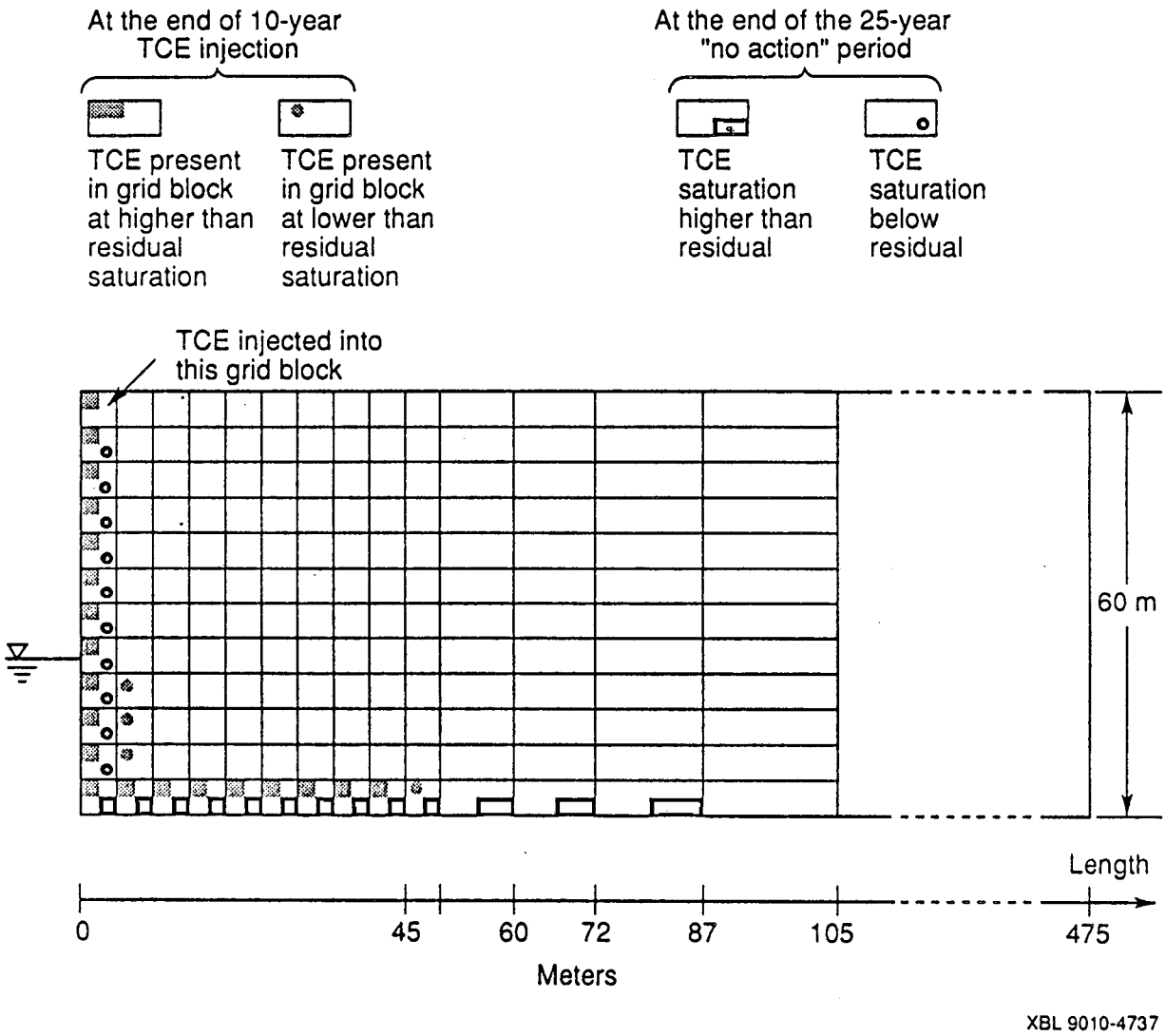

Figure 2. Distribution of separate-phase TCE at the end of (a) 10-year injection period and (b) 25-year "no action" period.

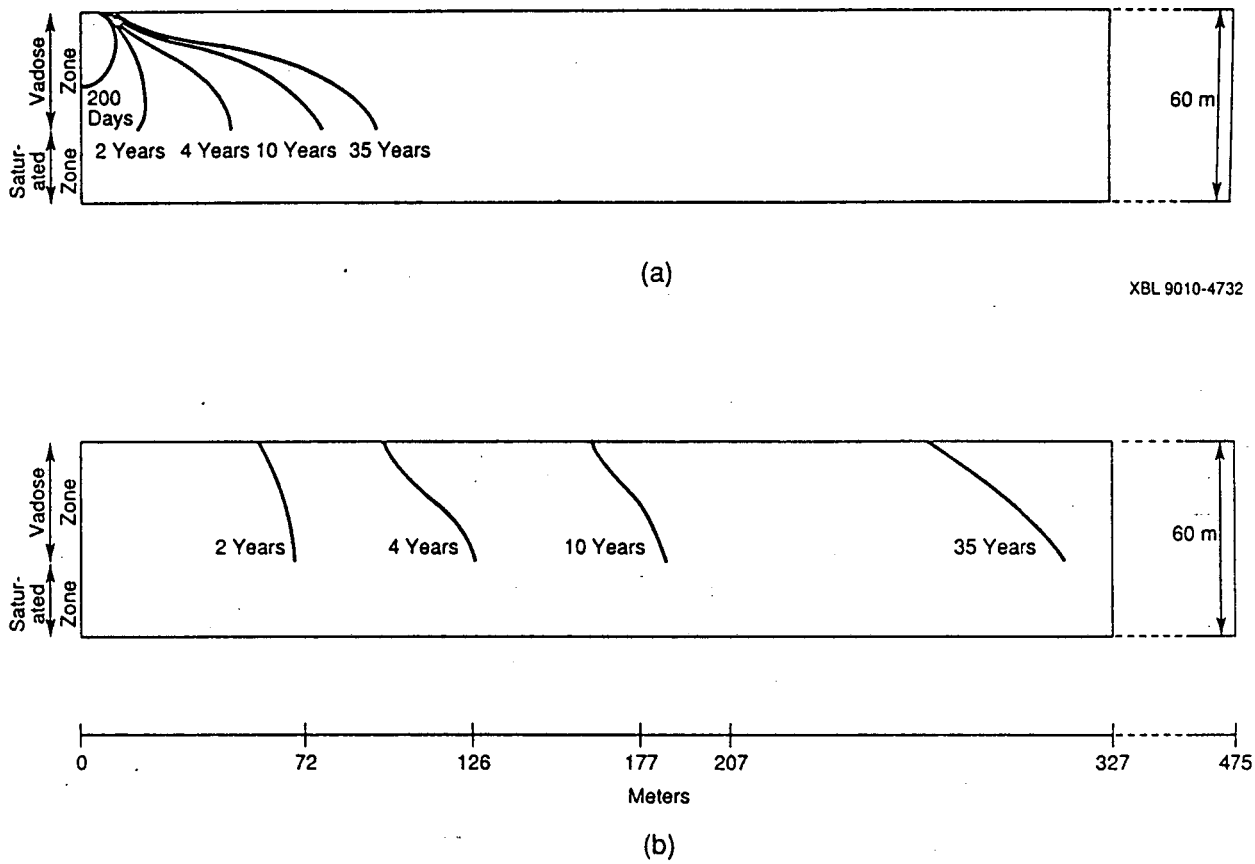

Figure 3. Locations of the vadose zone (a) $C_g^{TCE} = 0.1\ kg/m^3$, and (b) $C_g^{TCE} = 5 \times 10^{-5}\ kg/m^3$ contour at various times since the beginning of TCE injection.

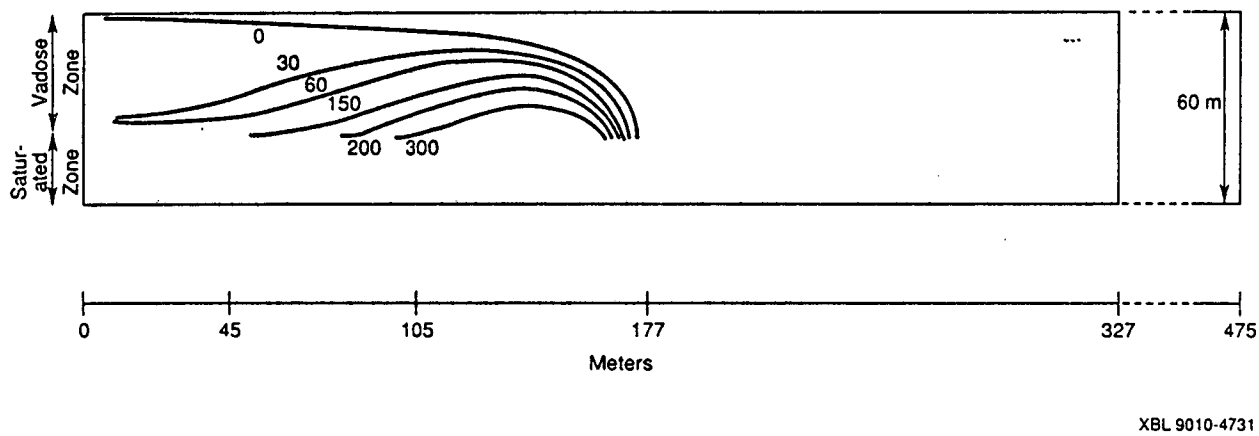

Figure 4. Locations of the vadose zone $C_g^{TCE} = 1 \times 10^{-2}$ kg/m^3 contour at different times (in days) since the beginning of gas extraction.

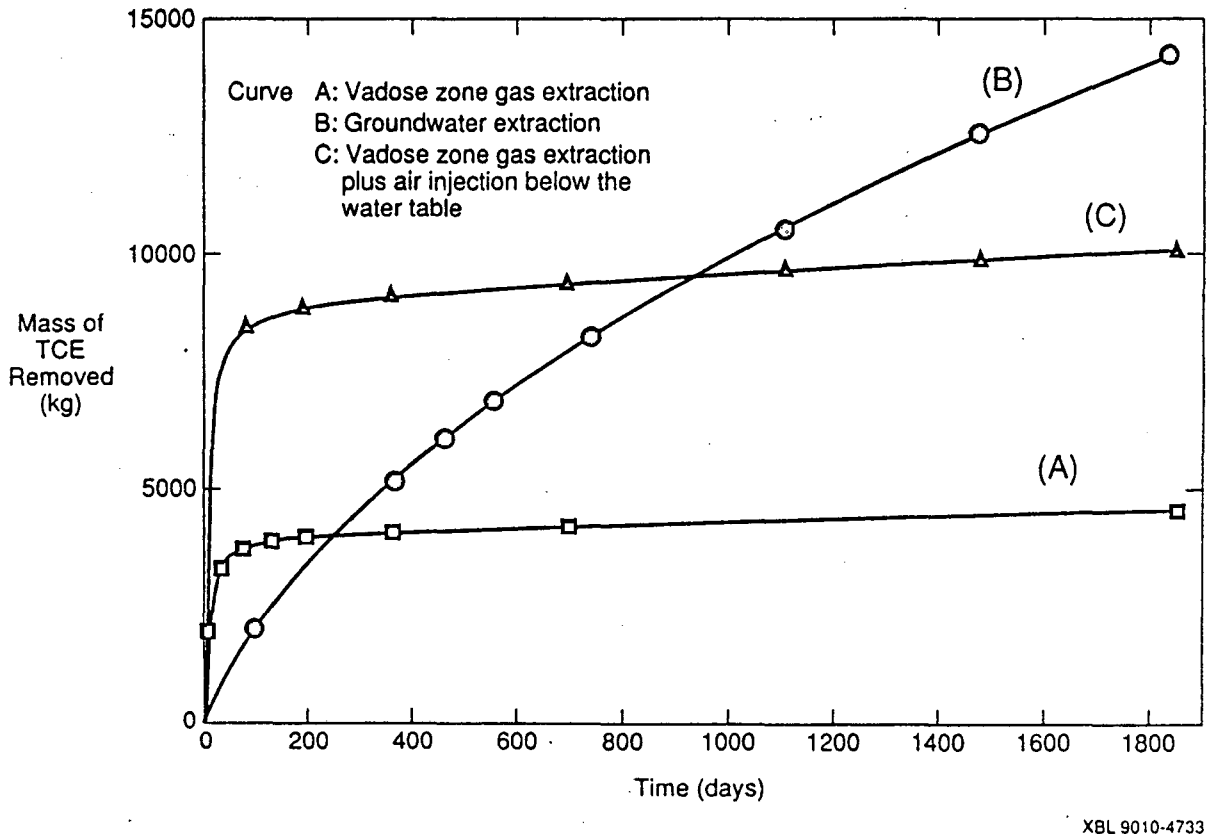

Figure 5. Cumulative TCE removal from the system for each of the three remediation schemes simulated.

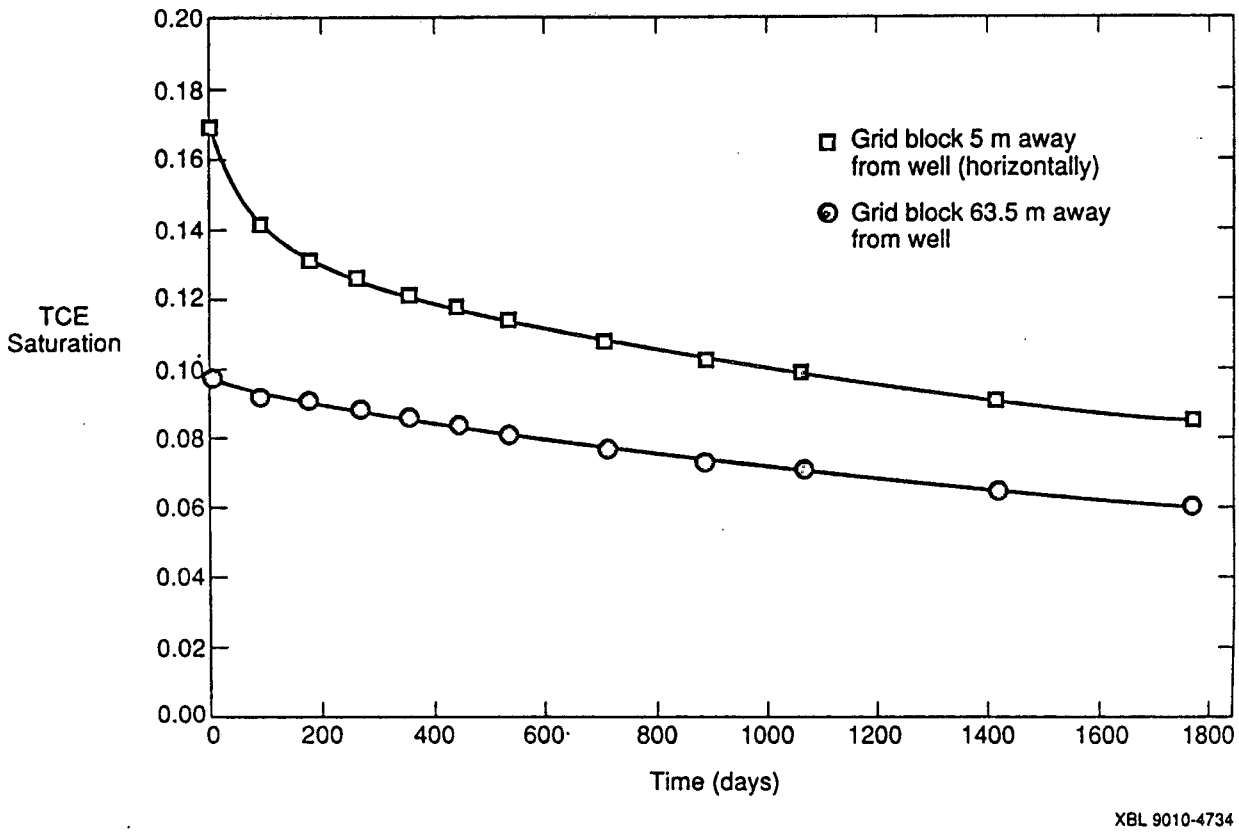

Figure 6. Plot of TCE saturation versus time at two different locations—groundwater extraction simulation.

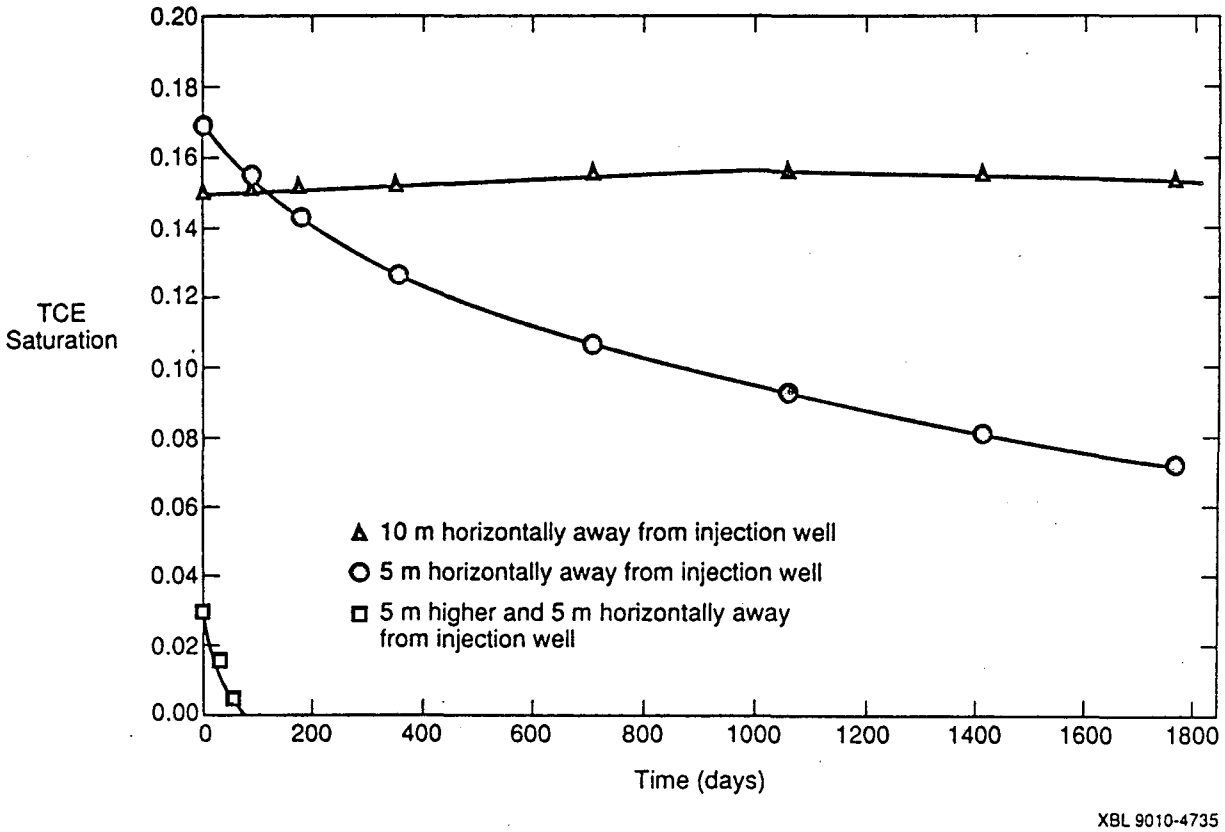

Figure 7. TCE saturations at three locations—vadose zone gas extraction plus air injection below the water table.

LAWRENCE BERKELEY LABORATORY
UNIVERSITY OF CALIFORNIA
INFORMATION RESOURCES DEPARTMENT
BERKELEY, CALIFORNIA 94720